International Journal of Mass Spectrometry 276 (2008) 127–135

Contents lists available at ScienceDirect

International Journal of Mass Spectrometry

journal homepage: www.elsevier.com/locate/ijms

Selecting fixed-charge groups for electron-based peptide dissociations A computational study of pyridinium tags

Thomas W. Chung, František Tureček*

Department of Chemistry, Bagley Hall, Box 351700, University of Washington, Seattle, WA 98195-1700, United States

ARTICLE INFO

Article history:
Received 12 February 2008
Received in revised form 19 April 2008
Accepted 22 April 2008
Available online 1 May 2008

Keywords:
Charge tags
Electron capture
Electron transfer
Excited states
Recombination energies

ABSTRACT

Fixed-charge groups based on pyridiniummethylcarboxamide moieties are analyzed by electronic structure theory calculations at combined B3LYP-PMP2 and CCSD(T) levels of theory to establish the ion recombination energies and thermodynamic and kinetic stability of radicals after electron capture. The fixed-charge pyridinium groups carry electron-donating and electron-withdrawing substituents and have higher recombination energies than protonated peptides, as modeled for $(GK+H)^+$ and $(GR+H)^+$. The pyridinium and peptide radicals formed by electron attachment have overlapping manifolds of electronic states that may allow for unidirectional or reversible intramolecular electron transfer in charge-tagged peptides. The pyridinium groups have moderate kinetic stabilities toward dissociation by N–CH_2 bond cleavage after electron attachment. Alkylammonium ions coordinated to 18-crown-6-ether show extremely low recombination energies and may represent a special kind of charge tags. Electron attachment to $[CH_3NH_3\ldots$18-crown-6-ether$]^+$ complex forms a dipolar species resembling an organic electride, in which the ionic alkylammonium core is surrounded by a crown-solvated electron.

1. Introduction

Electron-based methods of peptide dissociation, such as electron capture dissociation (ECD) [1], electron transfer dissociation (ETD) [2], electron capture induced dissociation (ECID) [3], and related methods [4], rely on charge reduction of singly or multiply charged peptide ions that converts even-electron precursors to odd-electron, peptide cation-radical, intermediates. Peptide radicals are often quite reactive and undergo various dissociations, such as losses of atoms (H) and small molecules (NH_3 and H_2O), side chain cleavages, and perhaps most important, peptide backbone cleavages that are useful for sequence determination [5]. Both the presence of residual charge and the electronic states that are accessed in the intermediates are important to affect the dissociations and to allow the products to be detected by mass spectrometry.

The role of electronic states gains importance in conjunction with the use of charge tags that are conjugated with the N-terminal or lysine amino groups [6] and used to increase the charge state of the peptide conjugate. Of necessity, electron attachment in the charge tag competes with electron capture in the protonated peptide moiety and can affect fragmentations of the charge-reduced species. So far, charge tags have been used in a mostly heuristic approach where the tag selection was guided by its chemical or other availability rather than electronic properties. For example, 2,2′-bipyridine was found to be an effective tag due to its substantial basicity and facile protonation by electrospray [7]. However, electron attachment to the protonated 2,2′-bipyridine group, albeit very efficient, was found to suppress peptide backbone dissociations [7]. The tris-(2,4,6-trimethoxyphenyl)phosphonium-methylcarboxamido group (TMPP) [8] has been used as a fixed-charge tag in peptides and shown to allow for efficient ECD [9]. In the presence of two TMPP groups, backbone dissociations were suppressed in dipeptides [10] but not in larger peptides [9], and the fixed-charge group was found to undergo substantial dissociation upon electron capture [9,10]. McLuckey and coworkers have investigated electron transfer dissociations of peptides that were charge-tagged with trimethylammonium groups [11]. Electron attachment to alkyl ammonium groups forms hypervalent radicals, which are only weakly bound [12] and undergo extensive dissociations that do not provide information about the peptide structure.

From the previous experimental work, it appears that the use of charge tags would benefit from a rational selection of the charged group. In addition to synthetic availability and favorable chemical properties, the main criteria for the selection of a charge tag are its electronic properties and stability following electron attachment. The electronic properties can be assessed from the intrinsic adia-

* Corresponding author. Tel.: +1 206 685 2041; fax: +1 206 685 3478.
E-mail address: turecek@chem.washington.edu (F. Tureček).

1387-3806/$ – see front matter © 2008 Elsevier B.V. All rights reserved.
doi:10.1016/j.ijms.2008.04.014

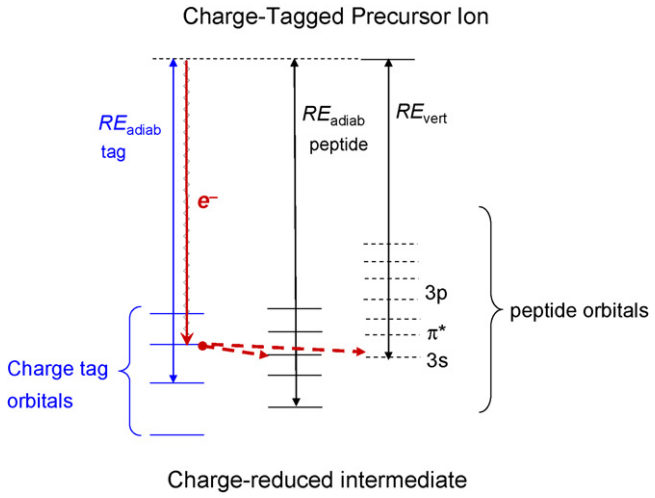

Scheme 1.

batic and vertical recombination energy of the charge tag, which are important for ECD and ECID, respectively. In ECD of trapped ions, the incoming electron follows a cascade of electronic states in the incipient reduced species [13a]. The electron recombination energy is converted to vibrational energy resulting in excitation of many internal degrees of freedom to drive dissociation, as shown by recent experiments [7]. The excitation energy in the peptide radical is expressed by the adiabatic ion-electron recombination energy. In ECID, the electron transfer occurs on a femtosecond time scale, and the accessible electronic states are characterized by vertical recombination energies.

Another important factor is the spacing and nodal properties of the ground and excited electronic states in the radical formed by electron attachment to the charge tag. Both the recombination energy and the manifold of electronic states in the reduced tag are likely to affect the electronic interactions with the protonated peptide moiety. Electronic states in peptide cation-radicals that are produced by electron capture or transfer have been shown to consist of dense manifolds of interspersed *n*s and *n*p Rydberg-like states where *n* is the principal quantum number determining the state nodality, and valence-type states, most notably amide π^* states. These were predicted to have high propensity for proton transfer [13] and have also been considered to engage in backbone dissociations [13,14]. Generic electronic state manifolds are sketched in Scheme 1 for states in the charge-tag (blue lines) accessed by electron capture and peptide orbitals, both vertical (dashed lines) and those developed after vibrational relaxation. Horizontal red arrows indicate intramolecular electron transfer between the matching energy levels in the charge-tag and peptide manifolds. Scheme 1 does not show rovibrational envelopes of each electronic state, which allow for substantial overlap of the rovibrational states of closely spaced electronic states in peptide cation-radicals.

Recently, cation-radicals derived from di- and tripeptides have been analyzed by electronic structure theory calculations and found to have near-degenerate electronic states of the n*s* Rydberg and π^* valence type [10]. It is now recognized that amide π^* states play an important role in backbone N–C_α bond dissociations that are used in peptide sequencing by ECD and ETD. Interactions of the electronic states in the charge tag with those in the peptide moiety can have substantial effects on reactivity. For example, quenching of peptide amide π^* states by intramolecular electron transfer [14,15] to an electronic state of the charge tag may have a deleterious effect on peptide backbone fragmentations [7].

1: R = H
2: R = 4-CH_3
3: R = 2,4,6-CH_3
4: R = 4-OCH_3
5: R = 4-$OSi(CH_3)_3$
6: R = 4-$N(CH_3)_2$
7: R = 2-CH_3, 4-$N(CH_3)_2$
8: R = 3-CH_3, 4-$N(CH_3)_2$
9: R = 4-CN

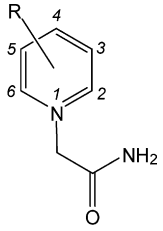

Here we report a computational analysis of a family of prospective charge tags that are based on substituted pyridinium groups, as represented by pyridiniummethylcarboxamides (**1**–**9**). The pyridiniummethylcarbonyl moiety can be introduced into the peptide molecule by *in situ* conjugation with a free amino group using

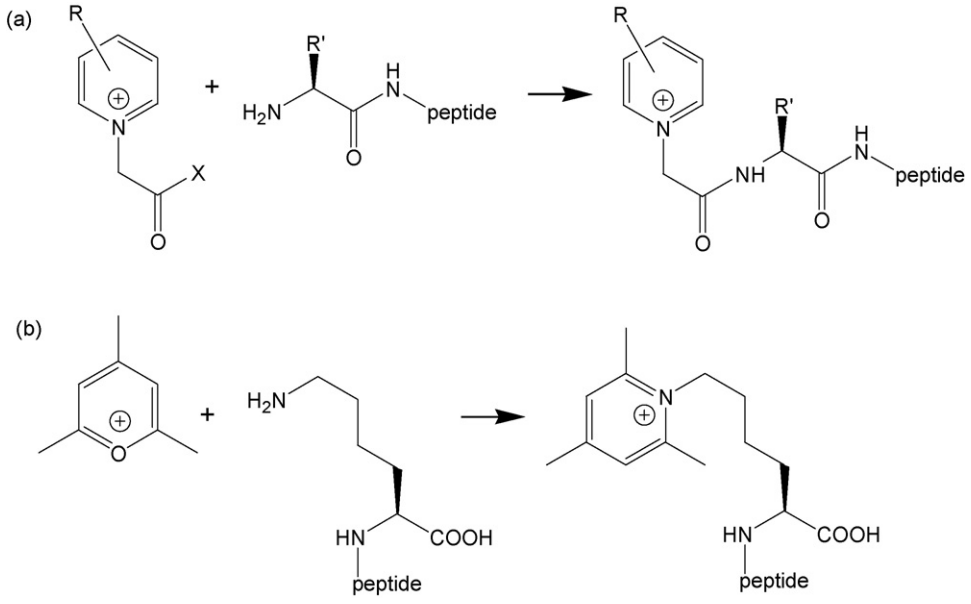

Scheme 2. .

the active ester coupling methodology. The active ester group, *N*-hydroxysuccinimide, tetrafluorophenyl, etc., is denoted as *X* in Scheme 2a [16]. Alternatively, substituted pyrrylium salts can be used to react with free lysine amino group to introduce *N*-alkyl pyridinium groups into the peptide molecule (Scheme 2b) [17]. The substituents (R) have been selected to range from electron-donating to electron-withdrawing in order to modify the electronic properties of the charged tag. At the same time, only substituents compatible with the tag conjugation chemistry were studied, which eliminated groups such as OH, NH_2, COOH, etc., due to competing reactions of the active ester with itself in solution. We investigate the recombination energies of the fixed-charge groups, their electronic excited states, and dissociation energetics of the radicals formed by electron attachment.

2. Calculations

Standard ab initio calculations were performed using the Gaussian 03 suite of programs [18]. Geometries were optimized with B3LYP [19] and the 6-31+G(d,p) basis set. The 6-31++G(d,p) basis set was used for open-shell systems. Tables of complete optimized structures are available from the corresponding author upon request. Local energy minima and transition states were characterized by harmonic frequency analysis to have the appropriate number of imaginary frequencies (zero for local minima and one for transition states). The calculated frequencies were scaled by 0.963 [20]. Improved energies were obtained by single-point calculations on the B3LYP-optimized geometries. The single-point calculations used B3LYP and Møller-Plesset perturbational theory truncated at second order with valence electrons only excitations (MP2 (frozen core)) and basis sets of triple-ζ quality that were furnished with multiple shells of polarization and diffuse functions, e.g., 6-311++G(2d,p), 6-311++G(3df,2p). For the largest molecular system studied here these basis sets comprised 672 and 922 primitive Gaussians, respectively. Spin unrestricted formalism was used for calculations of open-shell systems. Contamination by higher spin states was modest, as judged from the expectation values of the spin operator $\langle S^2 \rangle$ that were $\leq$0.76 for UB3LYP and $\leq$0.78 for UMP2 calculations for most radicals. The UMP2 energies were corrected by spin annihilation [21] that reduced the $\langle S^2 \rangle$ to close to the theoretical value for a pure doublet state (0.75). The single-point B3LYP and spin-projected MP2 energies were averaged according to the B3-PMP2 procedure [22] that results in cancellation of small errors inherent to both approximations and provides dissociation and transition state energies of improved accuracy as has been previously shown for a number of closed-shell and open-shell systems [23]. For selected systems single-point energies were also calculated using the coupled-cluster theory [24] with single, double, and

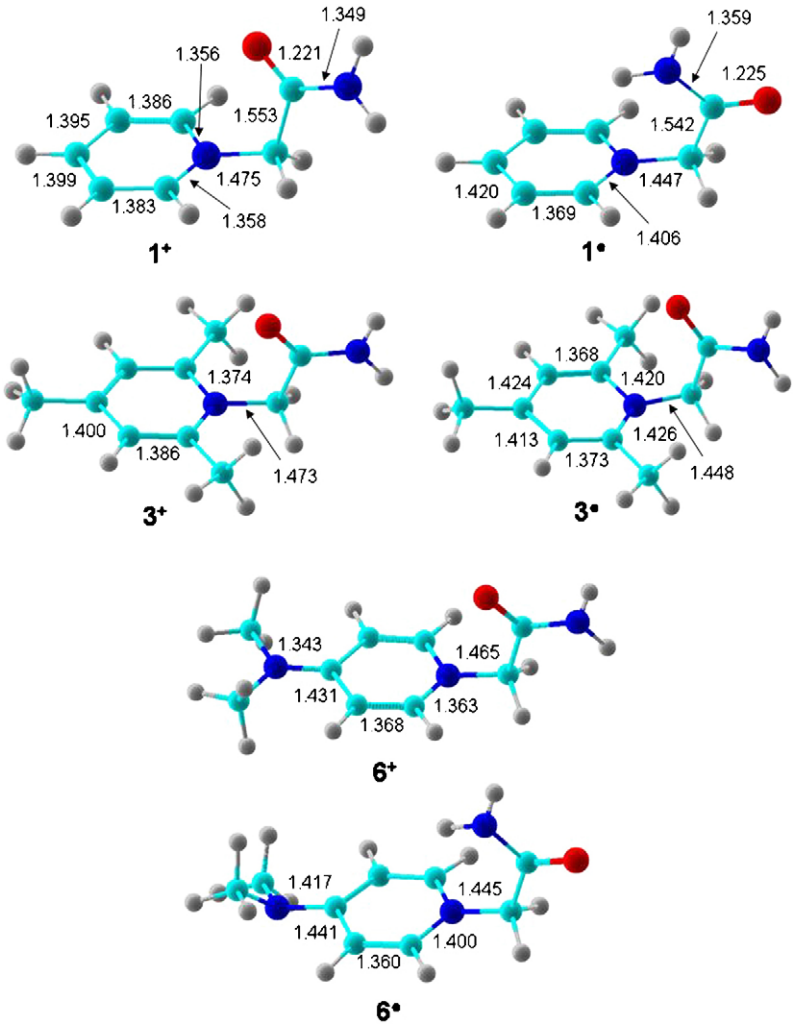

Fig. 1. B3LYP/6-31+G(d,p) optimized structures of $\mathbf{1}^+$, $\mathbf{1}^\bullet$, $\mathbf{3}^+$, $\mathbf{3}^\bullet$, $\mathbf{6}^+$, and $\mathbf{6}^\bullet$. Bond lengths are in Å.

disconnected triple excitations (CCSD(T)) [25], and the 6-31+G(d,p) basis set. The single-point energies were extrapolated to CCSD(T)/6-311++G(3df,2p) using the standard linear formula:

$$E[\text{CCSD(T)/6-311++G(3df, 2p)}] \approx E[\text{CCSD(T)/6-31+G(d, p)}] + E[\text{PMP2/6-311++G(3df, 2p)}] - E[\text{PMP2/6-31+G(d, p)}].$$

The recombination energies calculated with B3-PMP2 and the 6-311++G(2d,p) and 6-311++G(3df,2p) basis sets for $\mathbf{1}^+$, $\mathbf{2}^+$, $\mathbf{4}^+$, and $\mathbf{9}^+$ were, respectively, within 0.073 and 0.033 eV (root-mean square deviations) of the CCSD(T)/6-311++G(3df,2p) values. This indicates that the B3-PMP2 scheme, even when applied with the smaller basis set, gave reasonable estimates of recombination energies. This finding is encouraging, because CCSD(T) calculations of larger open-shell systems are prohibitively expensive and may require memory capacities which are beyond current computational capabilities. Excited state energies were calculated with time-dependent density functional theory [26] using B3LYP and the 6-311++G(2d,p) and 6-311+G(3df,2p) basis sets, which gave practically identical excitation energies. Atomic spin and charge densities were calculated using the natural population analysis (NPA) method [27].

3. Results and discussion

3.1. Optimized geometries

The molecular geometries of pyridinium cations and radicals are illustrated by the optimized structures of the simplest derivatives $\mathbf{1}^+$ and $\mathbf{1}^\bullet$ (Fig. 1). As expected, ion $\mathbf{1}^+$ has a planar pyridinium ring [28]. The *N*-methylcarboxamide group is rotated about the N–CH_2 bond at 68 degrees off the pyridinium ring plane, and the carbonyl oxygen points toward the ring. This conformation gives the energetically most favorable arrangement of the bond dipoles in the ion. Electron attachment to $\mathbf{1}^+$ gives radical $\mathbf{1}^\bullet$, which relaxes by adjusting several molecular parameters. Most notable of those are the ring N=C and C=C bond lengths which show different alternating patterns in $\mathbf{1}^+$ and $\mathbf{1}^\bullet$. In addition, the *N*-methylcarboxamide side-chain rotates following electron attachment to align the N–H and C=O bond dipoles with the electron-rich radical pyridinium ring (Fig. 1). Note that the pyridinium ring in $\mathbf{1}^\bullet$ is essentially planar and the *N*-atom shows only a minor (5°) pyramidization. The optimized geometry of $\mathbf{1}^\bullet$ has C_s symmetry. The ring bond-alternating pattern is also found in substituted pyridinium cations and radicals, e.g., the 2,4,6-trimethyl derivatives $\mathbf{3}^+$ and $\mathbf{3}^\bullet$. However, the conformation of the side chain depends on the ring substituents and prefers a carbonyl-in orientation in both $\mathbf{3}^+$ and $\mathbf{3}^\bullet$. The reason for this is probably a combination of polar and steric effects. In the absence of substituents in the *ortho* ring positions, the side-chain conformations are as in $\mathbf{1}^+$ and $\mathbf{1}^\bullet$, as shown for $\mathbf{6}^+$ and $\mathbf{6}^\bullet$ (Fig. 1) and likewise for the other derivatives.

3.2. Recombination energies

The vertical recombination energies (RE_{vert}, Table 1) of $\mathbf{1}^+$–$\mathbf{9}^+$ show expected substituent electronic effects in that the σ and π-electron-donating groups in the ring lower the recombination energies, whereas the π-electron attracting CN group in $\mathbf{9}^+$ increases it, both relative to the unsubstituted pyridinium system in $\mathbf{1}^+$. The vertical recombination energies range between 3.35 eV for R = 2–CH_3,4-N(CH_3)$_2$ ($\mathbf{7}^+$) to 5.39 eV for R=CN ($\mathbf{9}^+$). The adiabatic recombination energies follow the same trend ranging from 3.97 to 5.65 eV, with $\mathbf{7}^+$ and $\mathbf{9}^+$ again at opposite extremes (Table 1). With respect to lysine side-chain tagging (Scheme 2b), we also included in the present set *N*-ethyl-2,4,6-trimethylpyridinium ($\mathbf{10}^+$) as a model system. The RE_{adiab} for ion $\mathbf{10}^+$ (4.37 eV) is similar to that of $\mathbf{3}^+$ (Table 1).

The differences in the relaxed geometries of pyridinium cations and radicals lead to Franck–Condon effects upon vertical electron attachment. The Franck–Condon effects, when expressed as $E_{FC} = |RE_{adiab} - RE_{vert}|$, are moderate, ranging between 0.2 and 0.65 eV, but show no obvious pattern depending on the recombination energies or nature of the substituents. Most of the vibrational excitation through E_{FC} stems from the different ring C=C and N=C bond lengths in the cations and radicals, which depend only weakly on the substituents in the present family of structures. The E_{FC} values are useful for estimations of vibrational excitation in radicals formed by collisional electron transfer as in ECID, and are relevant for radical dissociations, as discussed later.

Both the adiabatic and vertical recombination energies of pyridinium cations $\mathbf{1}^+$–$\mathbf{9}^+$ are greater than the intrinsic recombination energies of singly protonated peptides. These have been reported recently for dipeptides that were protonated at the N-terminus, which had RE_{adiab} = 3.71 eV and RE_{vert} = 2.77 eV [29] in (GG-NH_2 + H)$^+$, in the lysine side chain, which had RE_{vert} = 3.15 eV [10] in (GK + H)$^+$, or in the arginine side chain, which had RE_{adiab} = 3.75 eV and RE_{vert} = 2.81 eV [10] in (GR + H)$^+$. The data imply that in a peptide derivative that was charge-tagged with a pyridinium group, the ground electronic state following electron attachment would correspond to a pyridinium radical. However, the manifolds of electronic states located on the fixed-charge groups and on the peptide can

Table 1
Recombination energies of pyridinium charge tags

Substituents/ion	RE_{adiab}[a,b]			RE_{vert}[a,c]
	B3-PMP2 6-311++G(2d,p)	B3-PMP2 6-311++G(3df,2p)	CCSD(T)[d] 6-311++G(3df,2p)	B3-PMP2 6-311++G(3df,2p)
H ($\mathbf{1}^+$)	5.00	5.03	5.00	4.53
4-CH_3 ($\mathbf{2}^+$)	4.41	4.53	4.56	4.32
2,4,6-CH_3 ($\mathbf{3}^+$)	4.32	4.34	–	4.01
4-OCH_3 ($\mathbf{4}^+$)	4.30	4.33	4.30	3.94
4-OSi(CH_3)$_3$ ($\mathbf{5}^+$)	4.25	4.27	–	3.72
4-N(CH_3)$_2$ ($\mathbf{6}^+$)	4.08	4.10	–	3.66
2-CH_3, 4-N(CH_3)$_2$ ($\mathbf{7}^+$)	3.95	3.97	–	3.35
3-CH_3, 4-N(CH_3)$_2$ ($\mathbf{8}^+$)	4.09	4.11	–	3.46
4-CN ($\mathbf{9}^+$)	5.61	5.65	5.61	5.39
$\mathbf{10}^+$	4.34	4.37	–	-

[a] In units of eV.
[b] Including B3LYP/6-31+G(d,p) zero-point vibrational energies and referring to 0 K.
[c] Without ZPVE corrections.
[d] From effective single-point energies: E[CCSD(T)/6-311++G(3df,2p)] ≈ E[CCSD(T)/6-31+G(d,p)] + E[PMP2/6-311++G(3df,2p)] – E[PMP2/6-31+G(d,p)].

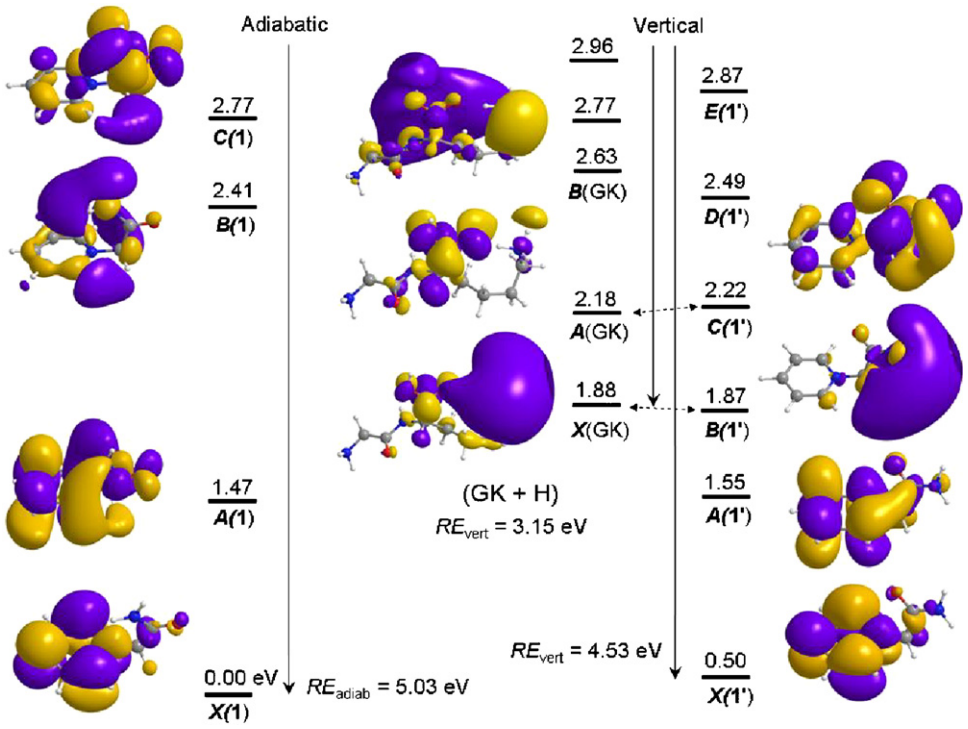

Fig. 2. Electronic state manifolds from TD-B3LYP/6-311++G(2d,p) calculations. Left manifold: vertical excitations from the optimized ***X*** state of **1**•. Middle manifold: vertical electron attachment to $(GK+H)^+$. Right manifold: vertical electron attachment to $\mathbf{1}^+$. The energies in eV refer to the ground state of the non-interacting [**1**. . .$(GK+H)]^•$ supersystem.

interact and result in intramolecular electron transfer. Such interactions are likely to depend on the relative energy levels for those states, as described and discussed next.

3.3. *Pyridinium. . .(GK + H) model*

Fig. 2 shows the molecular orbitals and electronic state manifolds in **1**• and a $(GK+H)^•$ fragment that were calculated at the same level of theory (TD-B3LYP/6-311++G(3df,2p). The leftmost manifold in Fig. 2 depicts the ground (***X***) and three lowest excited electronic states (***A***–***C***) of relaxed radical **1**•. The excitation energies (in eV) are for vertical electron excitations from the radical ground state. The rightmost manifold depicts the energy levels in **1**• that was formed by vertical electron attachment to ion $\mathbf{1}^+$ and retains the ion geometry. The center manifold shows the electronic levels in $(GK+H)^•$ radical formed by vertical electron attachment to $(GK+H)^+$. It should be noted that the recombination energies of doubly charged, pyridinium-tagged, peptide conjugates would be increased by coulomb effects of the remaining charge [10]. However, coulomb interactions are pair-wise and, considering that the charged groups are remote, the intrinsic recombination energies of the charge sites are affected to a similar extent. The lowest two electronic states of **1**•, denoted as ***X***(**1**) and ***A***(**1**) are represented by aromatic π orbitals in both relaxed and vertically formed radicals. The vertically formed **1**• is denoted as **1**′ in Fig. 2. The energies of these states are below the energy of the lowest state of the $(GK+H)^•$ moiety, denoted as ***X***(GK). Electron capture in the ***X***(**1**) and ***A***(**1**) states would trap the electron in the pyridinium group and possibly drive its dissociations, as discussed later. However, the electronic system of the charged peptide moiety would not be significantly perturbed to undergo radical-like dissociations which are typically observed on ECD/ETD of peptide cations. A recent report of ECD in a much larger system of tetradecapeptides that were charge-tagged on the N-terminus [7] corroborates this analysis.

On energy grounds, the ***B*** and higher electronic states in **1** allow for electron transfer between the peptide and charge-tag manifolds. However, the ***X***(GK) state is not a local potential energy minimum and spontaneously undergoes highly exothermic (ΔH_{rxn} = 1.09 eV, 105 kJ mol^{-1}) [10] proton migration to form a dihydroxycarbinyl radical that can further trigger a facile N–C_α bond dissociation [10,30]. Hence, both electron attachment in and intramolecular transfer to the ***X***(GK) state is predicted to initiate peptide isomerization followed by backbone dissociations. The ***A***(GK) state is represented by a π^* orbital that gives the state a zwitterionic character with a negatively charged $^-$O–C•–OH group and a positively charged ε-NH_3 group. Such states are predicted to undergo exothermic proton transfer forming again weakly bound ketyl radicals [13]. This analysis indicates that electron transfer to the reactive peptide states is more or less unidirectional; in other words, peptide states accessed by electron capture are unlikely to be depleted by electron transfer to the charge tag, even if the transfer is exothermic.

The previous discussion does not address the difficult question of cross-sections for electron capture in the various electronic states of multiply-charge peptide conjugates and also the cross-sections and mechanisms for electron transfer between the states. Simons and coworkers have recently analyzed this question with a simple model and concluded that electron transfer is more likely to occur by a through-bond mechanism than by a through-space one [15]. However, calculations of quantitatively accurate cross-sections for intramolecular electron transfer are currently beyond our capabilities in charge-tagged peptides [15].

3.4. *Pyridinium. . .(GR + H) model*

The above energy analysis was extended to charge tags that had lower recombination energies providing a closer match with those in the peptide moiety, and also to a (GR + H) peptide model that differs in its electronic structure and reactivity from (GK + H). The

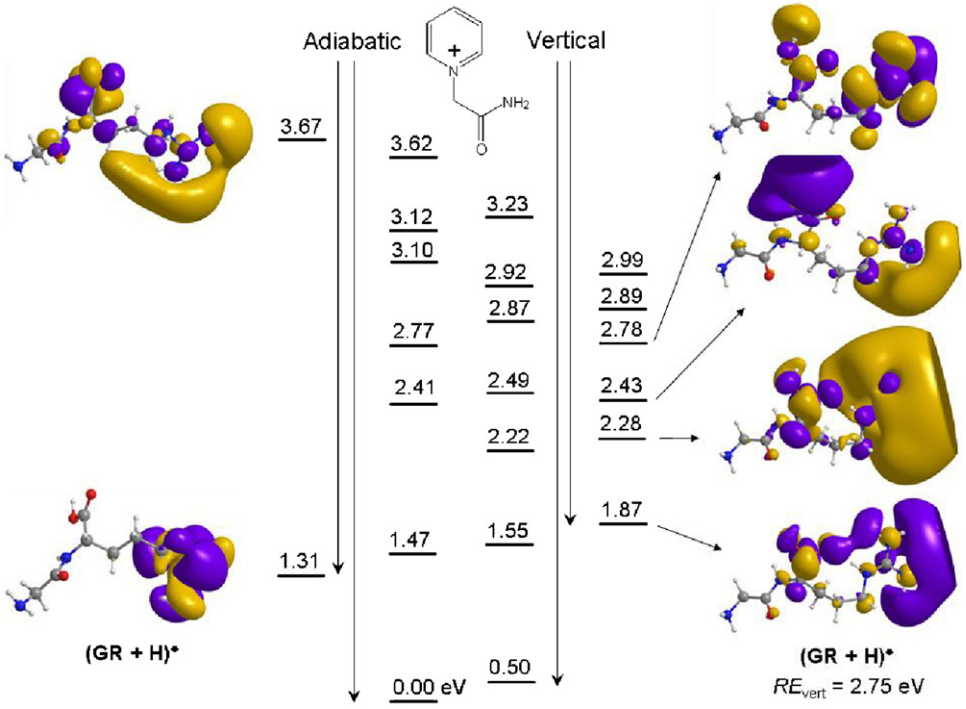

Fig. 3. Electronic state manifolds from TD-B3LYP/6-311++G(2d,p) calculations. Left manifold: vertical excitations from the optimized ***X*** state of (GR+H)• radical. Middle manifold: vertical and adiabatic electron attachment to $\mathbf{1}^+$. Right manifold: vertical electron attachment to $(GR+H)^+$. The energies in eV refer to the ground state of the non-interacting [**1**...(GR+H)]• supersystem.

pyridinium...(GR+H) system is analyzed first. Fig. 3 shows the excited state manifolds in **1**•, **1**′ and (GR+H)• formed by vertical electron attachment and after relaxation to the potential energy minimum of the radical. The energy scale (eV) is anchored to the ground electronic state of **1**•. The ground electronic state of (GR+H)• lies 1.3–1.9 eV above the ***X*** state of **1**• indicating that the ground state of a [pyridinium...(GR+H)]• conjugate will have the odd-electron mainly within the pyridinium moiety. There is substantial overlap of the energy manifolds for vertically formed (GR+H)• and the ***A*** and higher states of **1**• and **1**′. This indicates an energetically possible electron transfer from an initial ***A*** or higher states in **1**• to the electronic states of the peptide. Again, the cross-sections for such transfers are not obvious and will depend on the structure of the conjugate. Note that the vertically formed (GR+H)• is likely to undergo geometry relaxation by unfolding of the arginine side chain. This has a major effect on the electronic states because it weakens the interaction between the guanidinium and carbonyl π-orbitals and increases the gap between the ***X*** and ***A*** states in relaxed (GR+H)• (Fig. 3). Side-chain unfolding in neutralized arginine radical requires rotational barriers on the order of 7–15 kJ mol^{-1} and is expected to be fast [31] with rate constants approaching 10^{12} s^{-1} [31], so that it can compete with reverse electron transfer to the charge tag.

3.5. 4-Dimethylaminopyridinium...(GK+H) and (GR+H) models

The 4-dimethylaminopyridinium charge tags show the lowest recombination energies of the present set (Table 1). Hence, the electronic states of 4-dimethylaminopyridinium radicals show the closest match with the states in the peptide moiety and are most likely to interact by electron transfer. The energy manifolds for relaxed 4-dimethylaminopyridinium radical (**6**•), vertically formed species (**6**′), and vertically formed (GK+H)•, and (GR+H)• are depicted in Fig. 4. The electronic energy scale in Fig. 4 is anchored to that of **6**•. The ***A*** and higher electronic states of **6**′ show substantial overlap with the manifolds of (GK+H)• and (GR+H)•. Interactions between those states are energetically possible. Geometry relaxation in both **6**• and (GR+H)• results in an increased spacing of the electronic states, which is expected to lower the probability for interaction and electron transfer. Geometry relaxation in both **6**• and (GR+H)• is due to conformational changes by rotations about single bonds. As noted above, such rotations have low activation energies and can be expected to be fast. Geometry relaxation in (GK+H)• occurs by proton migration on a barrier-free potential energy surface, and therefore is inherently fast. The energy analysis indicates that it is the electronic states accessed by electron capture that dominate the further development on the potential energy surface. Surface crossing is most probable in the initial geometry but becomes less facile as the charge-reduced groups relax.

3.6. Dissociations of pyridinium charge tags upon electron attachment

In addition to their ability to accept an electron, which is expressed by the recombination energies, an important property of the charge-tag is its stability in the reduced form. By analogy with other pyridinium and heterocyclic radicals [28], we investigated the dissociation and transition state energies for cleavages of the N–CH_2 bonds in **1**•–**4**•, **6**•, and **9**• (Table 2). The calculated bond dissociation energies (ΔH_{diss}) indicate relatively facile dissociations, which are substantially endothermic only for the 4-cyanopyridinium radical **9**•. The pyridinium radicals are thermodynamically only weakly bound with respect to a loss of the pyridine ring. However, all N–CH_2 bond cleavages show activation energies in the range of 51–97 kJ mol^{-1} from B3-PMP2/6-311++G(3df,2p) calculations, and 67–114 kJ mol^{-1} from CCSD(T) calculations that were extrapolated to the same basis set (Table 2). The activation energies show a moderately tight linear correlation

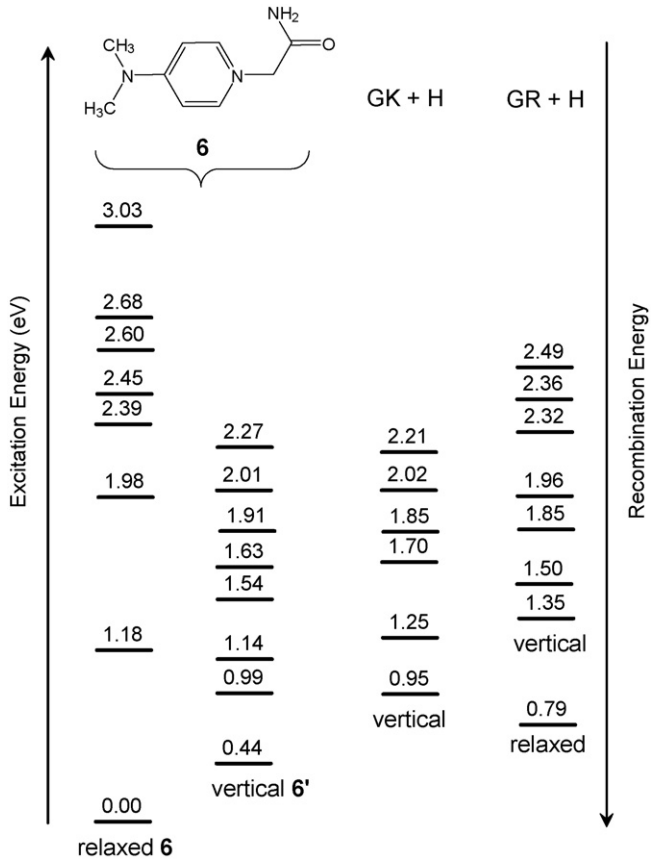

Fig. 4. Electronic state manifolds (eV) for **6,**• (GK+H),• and (GR+H)• from TD-B3LYP/6-311++G(2d,p) calculations.

with the bond dissociation energies, $E_{TS} = 0.774\Delta H_{diss} + 59.5$, with a correlation coefficient of $r^2 = 0.983$ for the current set of six values. From that we conclude that following electron attachment the pyridinium groups are kinetically stabilized. The TS energies for N–CH_2 bond cleavages are somewhat greater than those for N–C_α bond dissociations in peptide radicals. Hence, peptide conjugates can be expected to retain pyridinium groups upon electron capture, and unfavorable competition between peptide backbone dissociations and tag loss is not expected. The N–CH_2 bond in derivative **10**• shows a somewhat greater thermodynamic stability than the same bond in **3**•. The activation energy for the ethyl radical loss from **10**• (83 kJ mol^{-1}) is greater than that for the analogous dissociation in **3**•. This indicates that charge tags in the lysine side chains might be less susceptible to dissociation upon electron capture or transfer.

3.7. Auxiliary charge tags versus peptide charge insulators

The previous analysis disclosed some of the desirable properties of peptide charge tags. An ideal tag would not trap an electron in a non-reactive electronic state to hamper peptide fragmentation. At the same time, electron attachment to the tag should initiate efficient intramolecular electron transfer to the charged peptide moiety without inducing tag fragmentation. Owing to the very low recombination energies of charged peptide groups (vide supra), the options for ideal charge tags are limited. For example, alkylammonium tags have low recombination energies [12], but the radicals derived there from undergo facile dissociations by N–H and C–N bond cleavages that occur in the ground and excited electronic states [12]. Other charged groups, for example, guanidinium, $^+C(NH_3)_3$, and diaminohydroxycarbonium, $^+C(OH)(NH_2)_2$, have extremely low recombination energies, but the electron superrich radicals derived there from are weakly bound and readily dissociate [32].

A possible clue could be inferred from the extremely low recombination energies of alkylammonium cations that are coordinated to polydentate ligands. For example, a complex of methylammonium cation with 18-crown-6-polyether is calculated to have a recombination energy of $RE_{adiab} = 1.74$ eV to be compared to that for $CH_3NH_3^+$, $RE_{adiab} = 4.31$ eV (both from B3-PMP2/6-311++G(2d,p) calculations) [12b]. Attaching an 18-crown-6-polyether ligand to a peptide lysine or N-terminal ammonium group should result in a substantial lowering of the intrinsic recombination energy. This is equivalent to hoisting the electronic state manifold of the coordinated ammonium above that of other charged groups in the peptide and effectively insulating it from electron attachment. The insulating effect of the ligand is illustrated by the analysis of electronic states in the [CH_3NH_3 + 18-crown-6-polyether]• complex (Fig. 5). This shows the six lowest electronic states of the neutral complex to be represented by symmetry-adjusted s, p, and d Rydberg orbitals. The orbitals indicate that the unpaired electron density is delocalized about the crown-ether ring, but not within the ammonium group, as is typical for free ammonium radicals [12a,b]. The [CH_3NH_3 + 18-crown-6-polyether]• complex can be compared to an electride [33] having an ionic ammonium core and an outside crown-ether solvated electron. This is substantiated by the calculated atomic spin and charge densities, which show <2% of spin density and 0.57 positive charge at the ammonium group, whereas the crown ether carries 63% of spin density and −0.50 negative charge in the ground electronic state. The remaining 35% of spin density is at the methyl group. Since dissociations of ammonium radicals are triggered by interactions of the unpaired electron with the valence bond ones [12,13,34], the insulating effect of the crown ether in ammonium complexes can provide stabilization to the coordinated ammonium group. A recent report on electron transfer

Table 2
Dissociation and transition state energies for N–C bonds in substituted pyridinium–CH_2CONH_2 radicals

Radical	ΔH_{diss}[a,b]			E_{TS}[c]		
	B3-PMP2 6-311++G(2d,p)	B3-PMP2 6-311++G(3df,2p)	CCSD(T)[d] 6-311++G(3df,2p)	B3-PMP2 6-311++G(2d,p)	B3-PMP2 6-311++G(3df,2p)	CCSD(T)[d] 6-311++G(3df,2p)
1	31	36	51	86	90	103
2	−10	2	23	46	58	76
3	−15	−12	–	47	51	–
4	−10	−6	9	52	55	67
6	6	9	–	67	70	–
9	47	51	66	93	97	114

[a] In kJ mol^{-1}.
[b] Bond dissociation energies including B3LYP/6-31++G(d,p) zero-point vibrational energies and referring to 0 K.
[c] Transition state energies including B3LYP/6-31++G(d,p) zero-point vibrational energies.
[d] From effective single-point energies: E[CCSD(T)/6-311++G(3df,2p)] ≈ E[CCSD(T)/6-31+G(d,p)] + E[PMP2/6-311++G(3df,2p)] − E[PMP2/6-31+G(d,p)].

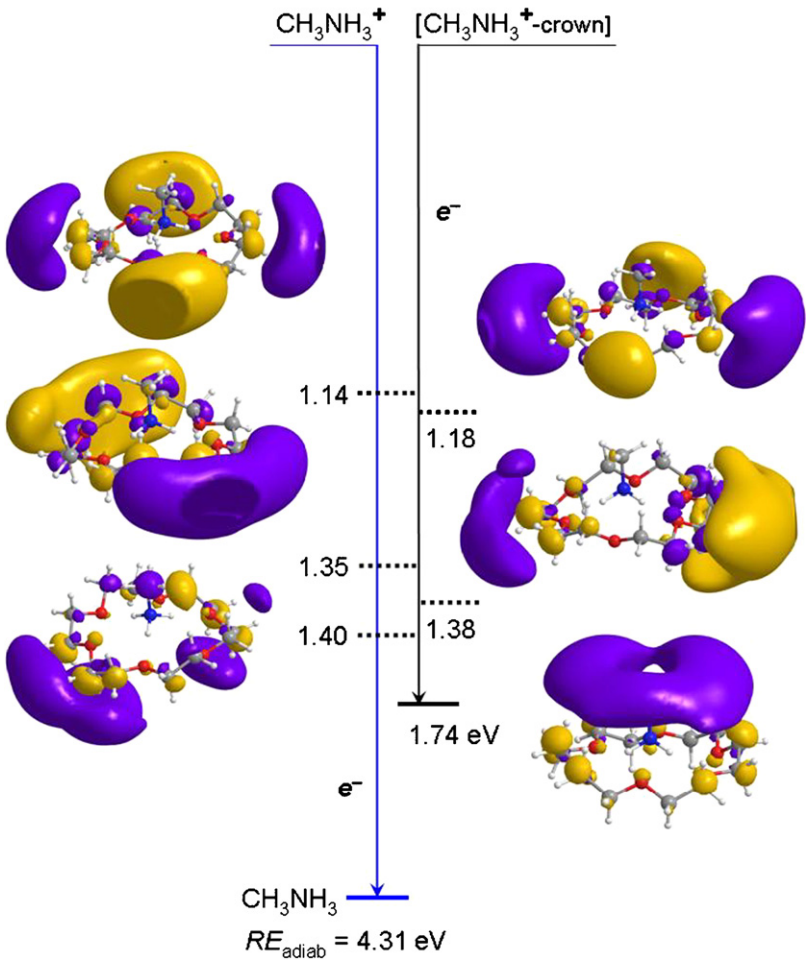

Fig. 5. Electronic state manifold for the $[CH_3NH_3 + 18\text{-crown-6-ether}]^{\bullet}$ complex showing recombination energies (in eV) for electron capture in the ***X***–***E*** states of the complex and the ***X*** state of $CH_3NH_3^{\bullet}$.

dissociations of doubly protonated dipeptide (KK)-18-crown-6-ether complexes [35] found practically no fragmentation in the lysine side chain in line with our theoretical analysis.

4. Conclusions

Fixed-charge pyridinium cations are calculated to have recombination energies in the range of 3.97–5.65 eV and can be used as charge tags in peptide ions for electron-based dissociation. The excited electronic states of pyridinium charge tags overlap with the ground and excited states of protonated lysine and arginine residues, as modeled for $(GK + H)^+$ and $(GR + H)^+$ dipeptide cations. The effect of the charge tag on electron capture and transfer dissociations of the peptide moiety depends on the overlap of the local electronic states and cross-sections for electron transfer between them. The optimum selection of the most effective charge tag can be guided by the present calculations, but needs to be tested by experiments with derivatized peptide ions. Complexation with crown ethers of peptide lysine ammonium groups represents an interesting mode of tagging due to the insulation of the coordinated ammonium group from the attached electron.

Acknowledgements

Support by grants from the National Science Foundation (CHE-0349595 CHE-0342956 and CHE-0750048) is gratefully acknowledged.

References

[1] R.A. Zubarev, N.L. Kelleher, F.W. McLafferty, J. Am. Chem. Soc. 120 (1998) 3265.
[2] (a) J.J. Coon, B. Ueberheide, J.E.P. Syka, D.D. Dryhurst, J. Ausio, J. Shabanowitz, D.F. Hunt, Proc. Natl. Acad. Sci. U.S.A. 102 (2005) 9463;
(b) S.J. Pitteri, P.A. Chrisman, J.M. Hogan, S.A. McLuckey, Anal. Chem. 77 (2005) 1831.
[3] P. Hvelplund, B. Liu, S. Brondsted-Nielsen, S. Tomita, Int. J. Mass Spectrom. 225 (2003) 83.
[4] F. Tureček, Top. Curr. Chem. 225 (2003) 77.
[5] H.J. Cooper, K. Hakansson, A.G. Marshall, Mass Spectrom. Rev. 24 (2005) 201.
[6] Z.-H. Huang, J. Wu, K.D.W. Roth, Y. Yang, D.A. Gage, J.T. Watson, Anal. Chem. 69 (1997) 137.
[7] J.W. Jones, T. Sasaki, D.R. Goodlett, F. Tureček, J. Am. Soc. Mass Spectrom. 18 (2007) 432.
[8] N. Sadagopan, J.T. Watson, J. Am. Soc. Mass Spectrom. 11 (1999) 107.
[9] J. Chamot-Rooke, G. van der Rest, A. Dalleu, A. Bay, J. Lemoine, J. Am. Soc. Mass Spectrom. 18 (2007) 1405.
[10] J. Chamot-Rooke, C. Malosse, G. Frison, F. Tureček, J. Am. Soc. Mass Spectrom. 18 (2007) 2146.
[11] (a) H.P. Gunawardena, L. Gorenstein, D.E. Erickson, Y. Xia, S.A. McLuckey, Int. J. Mass Spectrom. 265 (2007) 130;
(b) Y. Xia, H.P. Gunawardena, D.E. Erickson, S.A. McLuckey, J. Am. Chem. Soc. 129 (2007) 12232.
[12] (a) S.A. Shaffer, F. Turecek, J. Am. Chem. Soc. 116 (1994) 8647;
(b) C. Yao, F. Tureček, Phys. Chem. Chem. Phys. 7 (2005) 912.
[13] (a) E.A. Syrstad, F. Tureček, J. Am. Soc. Mass Spectrom. 16 (2005) 208;
(b) C. Yao, E.A. Syrstad, F. Tureček, J. Phys. Chem. A 111 (2007) 4167.
[14] M. Sobczyk, I. Anusiewicz, J. Berdys-Kochanska, A. Sawicka, P. Skurski, J. Simons, J. Phys. Chem. A 109 (2005) 250.
[15] (a) M. Sobczyk, J. Simons, Int. J. Mass Spectrom. 253 (2006) 274;
(b) M. Sobczyk, D. Neff, J. Simons, Int. J. Mass Spectrom. 269 (2008) 149.
[16] K.D.W. Roth, Z.H. Huang, N. Sadagopan, J.T. Watson, Mass Spectrom. Rev. 17 (1998) 255.

[17] R.S. Johnson, S.A. Martin, K. Biemann, Int. J. Mass Spectrom. Ion Proces. 86 (1988) 137.
[18] M.J. Frisch, G.W. Trucks, H.B. Schlegel, G.E. Scuseria, M.A. Robb, J.R. Cheeseman, J.A. Montgomery Jr., T. Vreven, K.N. Kudin, J.C. Burant, J.M. Millam, S.S. Iyengar, J. Tomasi, V. Barone, B. Mennucci, M. Cossi, G. Scalmani, N. Rega, G.A. Petersson, H. Nakatsuji, M. Hada, M. Ehara, K. Toyota, R. Fukuda, J. Hasegawa, M. Ishida, T. Nakajima, Y. Honda, O. Kitao, H. Nakai, M. Klene, X. Li, J.E. Knox, H.P. Hratchian, J.B. Cross, C. Adamo, J. Jaramillo, R. Gomperts, R.E. Stratmann, O. Yazyev, A.J. Austin, R. Cammi, C. Pomelli, J.W. Ochterski, P.Y. Ayala, K. Morokuma, G.A. Voth, P. Salvador, J.J. Dannenberg, V.G. Zakrzewski, S. Dapprich, A.D. Daniels, M.C. Strain, O. Farkas, D.K. Malick, A.D. Rabuck, K. Raghavachari, J.B. Foresman, J.V. Ortiz, Q. Cui, A.G. Baboul, S. Clifford, J. Cioslowski, B.B. Stefanov, G. Liu, A. Liashenko, P. Piskorz, I. Komaromi, R.L. Martin, D.J. Fox, T. Keith, M.A. Al-Laham, C.Y. Peng, A. Nanayakkara, M. Challacombe, P.M.W. Gill, B. Johnson, W. Chen, M.W. Wong, C. Gonzalez, J.A. Pople, Gaussian 03, Revision B. 05, Gaussian Inc., Pittsburgh, PA, 2003.
[19] (a) A.D. Becke, J. Chem. Phys. 98 (1993) 1372;
(b) A.D. Becke, J. Chem. Phys. 98 (1993) 5648.
[20] G. Rauhut, P. Pulay, J. Phys. Chem. 99 (1995) 3093.
[21] (a) H.B. Schlegel, J. Chem. Phys. 84 (1986) 4530;
(b) I. Mayer, Adv. Quant. Chem. 12 (1980) 189.
[22] F. Tureček, J. Phys. Chem. A 102 (1998) 4703.
[23] (a) F. Tureček, J.K. Wolken, J. Phys. Chem. A 103 (1999) 1905;
(b) F. Tureček, M. Polášek, A.J. Frank, M. Sadílek, J. Am. Chem. Soc. 122 (2000) 2361;
(c) M. Polášek, F. Tureček, J. Am. Chem. Soc. 122 (2000) 9511;
(d) P.R. Rablen, J. Am. Chem. Soc. 122 (2000) 357;
(e) P.R. Rablen, J. Org. Chem. 65 (2000) 7930;
(f) P.R. Rablen, K.H. Bentrup, J. Am. Chem. Soc. 125 (2003) 2142;
(g) M. Hirama, T. Tokosumi, T. Ishida, J. Aihara, Chem. Phys. 305 (2004) 307.
[24] J. Čížek, J. Paldus, L. Šroubková, Int. J. Quant. Chem. 3 (1969) 149.
[25] G.D. Purvis III, R.J. Bartlett, J. Chem. Phys. 76 (1982) 1910.
[26] R.E. Stratmann, G.E. Scuseria, M.J. Frisch, J. Chem. Phys. 109 (1988) 8218.
[27] A.E. Reed, R.B. Weinstock, F. Weinhold, J. Chem. Phys. 83 (1985) 735.
[28] V.Q. Nguyen, F. Tureček, J. Mass Spectrom. 32 (1997) 55.
[29] F. Tureček, E.A. Syrstad, J. Am. Chem. Soc. 125 (2003) 3353.
[30] S. Hayakawa, M. Hashimoto, H. Matsubara, F. Tureček, J. Am. Chem. Soc. 129 (2007) 7936.
[31] S. Hayakawa, H. Matsubara, S. Panja, P. Hvelplund, S.B. Nielsen, X. Chen, F. Tureček, J. Am. Chem. Soc. 130 (2008), doi:10.1021/ja800207x.
[32] C. Hao, J.L. Seymour, F. Tureček, J. Phys. Chem. A 112 (2007) 8829.
[33] (a) J.L. Dye, Science 301 (2003) 607;
(b) J.L. Dye, M.J. Wagner, G. Overney, R.H. Huang, T.F. Nagy, D. Tománek, J. Am. Chem. Soc. 118 (1996) 7329.
[34] A.I. Boldyrev, J. Simons, J. Chem. Phys. 97 (1992) 6621.
[35] A.I.S. Holm, P. Hvelplund, U. Kadhane, M.K. Larsen, B. Liu, S.B. Nielsen, S. Panja, J.M. Pedersen, T. Skrydstrup, K. Støchkel, E.R. Williams, E.S. Worm, J. Phys. Chem. A 111 (2007) 9641.